

Subharmonic autoresonance of the diocotron mode*

L. Friedland

Racah Institute of Physics, Hebrew University of Jerusalem, 91904, Jerusalem, Israel

J. Fajans[†] and E. Gilson

Department of Physics, University of California, Berkeley, Berkeley, California 94720-7300

(Received 8 November 1999; accepted 13 December 1999)

This paper investigates the excitation and control of the driven $l=1$ diocotron mode in a pure electron plasma by adiabatic passage through higher order resonances. The excitation takes place when the driving frequency ω_d is swept such that its n^{th} harmonic passes through the linear diocotron mode frequency ω_0 ; $\omega_d \approx \omega_0/n$, $n=2,3,\dots$. Once past the resonant region, the mode enters the autoresonant regime characterized by persisting phase locking and strong nonlinearities. The transition to autoresonance occurs provided that the driving amplitude exceeds a sharp threshold, which scales as $A^{3/(4n)}$, where $A/2\pi$ is the driving frequency chirp rate. The theory of these thresholds for $n=2$ and $n=3$ is developed and experimental results for $n=1,2,3,4$ and 5 are presented. © 2000 American Institute of Physics. [S1070-664X(00)90105-8]

I. INTRODUCTION

Autoresonance is an important phase locking phenomenon occurring in perturbatively-driven, nonlinear oscillatory systems. Its signature is persisting synchronization between the system and its drive when externally controlled parameters in the system (the driving frequency/wave vector, for example) vary in space and/or time. This continuing phase locking insures that the state of the system adiabatically self-adjusts to the varying external conditions, thereby allowing the excitation to be efficiently controlled. Applications of autoresonance are known in many branches of nonlinear physics; examples include particle accelerators,¹ molecular physics,^{2,3} nonlinear dynamics,⁴ nonlinear waves,^{5,6} and fluid dynamics.⁷ Recently, we have reported on the autoresonant excitation of the diocotron mode in a pure-electron plasma by passing through the fundamental resonance.^{8,9}

The $l=1$ diocotron mode comprises a magnetized electron column trapped in a Malmberg—Penning trap,¹⁰ which performs an azimuthal **EXB** rotation due to the electric field of the positive image charge induced on the grounded confining cylindrical wall (see Fig. 1). The angular frequency $\omega = \omega_0/(1-\rho^2)$ of the diocotron mode depends on the normalized mode amplitude $\rho = r/R$, (r being the radial position of the plasma and R being the radius of the cylindrical wall), where the linear response frequency $\omega_0 = 2c\lambda/BR^2$ is defined by the line charge density λ of the plasma column. If a sector of the confining wall is driven with an oscillating potential $V(t) = V_0 \cos \Psi(t)$, characterized by a slowly varying angular frequency $\omega_d(t) = d\Psi/dt \equiv \Psi_t$ then, when certain conditions are met,^{8,9} the diocotron mode phase locks to the drive as $\omega_d(t)$ increases in time and passes, at $t=t_0$, the fundamental linear resonance $\omega_d(t_0) = \omega_0$. Later the mode evolves in autoresonance; $\omega_0/(1-\rho^2(t)) \approx \omega_d(t)$ continuously. Thus $\rho(t) \approx [1 - \omega_0/\omega_d(t)]^{1/2}$ for $t > t_0$, and the mode

can be excited to large amplitudes simply by increasing the driving frequency. The process is reversible and the mode can be returned to its unexcited state by reversing the direction of variation of the driving frequency. The most difficult issue in autoresonance is the continuation of the initial phase locking in the system in transition to autoresonance. One finds that for a given chirp rate $A/2\pi = (1/2\pi)d\omega_d/dt$, the transition to autoresonance has a sharp threshold on the driving amplitude, namely $V_{0\text{th}} \sim A^{3/4}$.

In the present work we report on autoresonant control of the diocotron mode at higher order resonances, i.e., when the driving frequency is a fraction $\omega_d = \omega_0/n$, $n=2,3,\dots$ of the mode frequency. We shall refer to this phenomenon as the *subharmonic* autoresonance in contrast to the *fundamental* autoresonance at $n=1$. Subharmonic autoresonance was recently studied in a driven dynamical system,¹¹ so this work is an application of similar ideas to driven non-neutral plasmas.

We proceed by presenting our experimental results. Our main finding is that, for $n=1,2,3,4,5$, the subharmonic¹² autoresonance phenomenon has a sharp threshold on the driving amplitude similar to that seen for fundamental autoresonance.^{8,9} The threshold scales with the driving frequency chirp rate $A/2\pi$ as

$$V_{0\text{th}} \sim A^{3/(4n)}. \quad (1)$$

This result is illustrated in Fig. 2, which shows both the experimental results and the scaling.

Qualitatively subharmonic autoresonance can be explained as follows: Driving at a subharmonic frequency yields a nonresonant linear response of $O(V_0)$ at the system's driving frequency ω_d . Then, the n^{th} order nonlinearity in either the diocotron mode, the driving field, or both yields an $O(V_0^n)$ response at frequency $n\omega_d$. The latter response serves as an effective drive of strength $V_{\text{eff}} \sim V_0^n$ at frequency $\omega_{\text{eff}}(t) = n\omega_d(t)$, and, when it passes the fundamental linear resonance point, i.e., when $\omega_{\text{eff}}(t_0) = \omega_0$ at some time t_0 , it excites autoresonance in the system. The threshold for this

*Paper HI 23 Bull. Am. Phys. Soc. **44**, 157 (1999).

[†]Invited speaker.

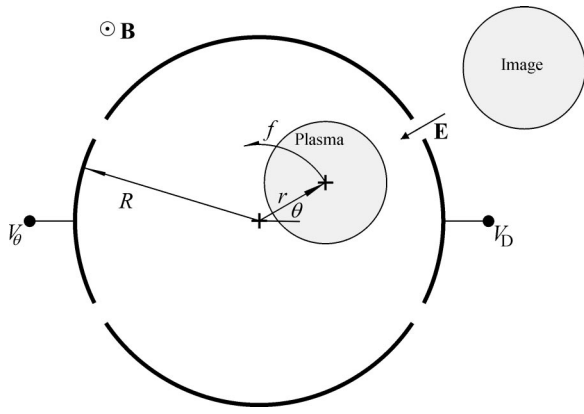


FIG. 1. Endview of the trap showing the confining wall at R , the plasma at angle θ , and distance r from the trap center, the plasma image, the image electric field \mathbf{E} , and the diocotron drift at frequency $\omega/2\pi$. For our experiments, $\omega_0/2\pi = 26.4$ kHz. The mode is detected by monitoring the image charge on the pickup sector V_θ and driven by applying a voltage to the drive sector V_D . Further details are given in Ref. 9.

excitation scales as $(V_{\text{eff}})_{\text{th}} \sim A^{3/4}$ similar to the fundamental autoresonance case. Returning to the original driving amplitude, V_0 , yields the subharmonic autoresonance threshold scaling, Eq. (1). Section II of the present work is devoted to the quantitative description of this threshold phenomenon. We shall see that the theory becomes increasingly complex as one considers higher and higher order resonances. Thus, we shall limit the theory to $n=2$ and some of the possible cases for $n=3$. We summarize our findings and present our conclusions in Sec. III.

II. THRESHOLD PHENOMENON

Consider the drifting plasma column shown in Fig. 1. The averaged transverse field acting on the plasma (we neglect the self field of the column) is given by the potential

$$\varphi(\rho, \theta) = -(\lambda/\beta) \ln(1 - \beta\rho^2) + \varphi_d(\rho, \theta), \quad (2)$$

where the first term represents the contribution of the image charge, and the factor β generalizes the equation to account

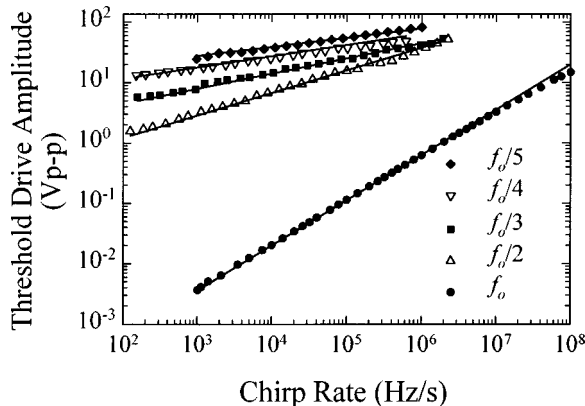


FIG. 2. Peak to peak threshold voltage $2V_{0\text{th}}$ vs the chirp rate $A/2\pi$, for the $n=1$ fundamental, and the $n=2,3,4,5$ subharmonics. The lines graph the scaling relations $V_{0\text{th}} \propto A^{3/(4n)}$, with the proportionalities fit to the data.

for a broad class of finite plasma length and radius corrections to the linear frequency.¹³ In our experiments, $\beta = 0.6$.⁹ The second term in Eq. (2),

$$\varphi_d(\rho, \theta) = V_0 \cos[\Psi(t)] \sum_{n=1}^{\infty} \alpha_n \rho^n \cos(n\theta), \quad (3)$$

is the driving potential in our cylindrical geometry (assuming, at this point, an infinite length driving sector). The coefficients α_n in Eq. (3) are given by the boundary conditions, i.e., $\alpha_n = [2/(n\pi)] \sin(n\theta_0)$, where $2\theta_0$ is the angular extent of the driving sector (see Fig. 1). Next we write the $\mathbf{E} \times \mathbf{B}$ drift evolution equations for our plasma in normalized Cartesian coordinates $X = \rho \cos \theta$ and $Y = \rho \sin \theta$, i.e., $X_t = -(c \partial \varphi / \partial Y) / (BR^2)$ and $Y_t = (c \partial \varphi / \partial X) / (BR^2)$, or

$$X_t = -\omega_0 Y / (1 - \beta\rho^2) - \epsilon \cos[\Psi(t)] \partial S / \partial Y, \quad (4)$$

$$Y_t = \omega_0 X / (1 - \beta\rho^2) + \epsilon \cos[\Psi(t)] \partial S / \partial X, \quad (5)$$

where $\epsilon = (cV_0)/(BR^2)$ is the normalized drive's amplitude, and $S(X, Y) = \sum_{n=1}^{\infty} \alpha_n s_n$, with each $s_n = \rho^n \cos(n\theta)$ simply related to X and Y . The three relations relevant to our analysis of subharmonic autoresonance in the system at $n=1,2,3$, are $s_1 = X$, $s_2 = X^2 - Y^2$, and $s_3 = X(X^2 - 3Y^2)$.

To study the evolution of our system under different driving conditions, we must analyze the slow, phase-locked solutions to Eqs. (4) and (5), which we can do using Whitham's averaged variational principle.¹⁴ We begin by constructing the Lagrangian,

$$L(X, X_t, Y, Y_t; t) = \frac{1}{2} (XY_t - X_t Y) + \frac{\omega_0}{2\beta} \ln(1 - \beta\rho^2) - \epsilon S \cos \Psi(t), \quad (6)$$

where ϵ is viewed as a small parameter. As shown below, the smallness of ϵ makes the autoresonance threshold a weakly nonlinear phenomenon. Consequently, we will expand the logarithm in Eq. (6) in powers of $\rho^2 = X^2 + Y^2$ up to ρ^4 , thereby preserving the weak nonlinearity of the diocotron mode. As the simplest illustration of applying Whitham's method to our problem, and to prepare to study subharmonic autoresonance, we first construct the averaged variational principle for fundamental autoresonance.

A. Fundamental autoresonance

In this case the angular driving frequency $\omega = d\Psi(t)/dt$ is an increasing function of time passing the linear mode frequency ω_0 at some time, say $t_0 = 0$. For simplicity, we shall assume a linear chirp, i.e., $\omega_d = \omega_0 + At$. We leave only the lowest order resonant component $s_1 \sim O(\rho)$ in S in the Lagrangian [Eq. (6)], and expand $\ln(1 - \beta\rho^2) \approx -\beta\rho^2 - \frac{1}{2}\beta^2\rho^4$. The resulting approximate Lagrangian is

$$L_1 = \frac{1}{2} (XY_t - X_t Y) - \frac{\omega_0}{4} (2\rho^2 + \beta\rho^4) - \epsilon \tilde{S}_1 \cos \Psi(t), \quad (7)$$

where $\tilde{S}_1 = \alpha_1 X$. Since the unperturbed ($\epsilon = 0$) problem yields a uniform azimuthal rotation of the plasma (the fast time scale in the problem) and the perturbation has a *slow*

parameter (the driving frequency), we seek a solution of the perturbed problem in the form $X = U[\Theta(t), t]$, $Y = V[\Theta(t), t]$, which is 2π -periodic in Θ and evolves on both slow and fast temporal scales. The explicit time dependence in U and V is assumed to be slow, but $\Theta(t)$ is the fast angle variable. At the same time, the angular frequency $\Omega = \dot{\Theta}_t$ is viewed as a slow function of time. Furthermore, we assume continuing phase locking in the system on the slow time scale, i.e., that the phase mismatch $\Phi = \Theta(t) - \Psi(t)$ between the mode and the drive remains bounded and slow. Whitham's method allows us to take advantage of the large difference between the above-mentioned time scales and, essentially, average out the fast scale. In the weakly nonlinear problem of interest we proceed by writing the driven solution by using the functional form of the unperturbed ($\epsilon = 0$) solution, i.e., $X = a \cos \Theta$ and $Y = a \sin \Theta$, where a is assumed to be slow. Thus, at this stage, we have transformed from X, Y to a new set of independent variables a, Θ , but also made explicit assumptions on the variation time scales of the new variables. These assumptions require *a posteriori* justification. Next, we write the interaction term in Eq. (7) as $-\epsilon \alpha_1 X \cos(\Theta - \Phi)$ and average our Lagrangian over the fast angle variable, i.e., calculate $\mathcal{L}_1 = (2\pi)^{-1} \int_0^{2\pi} L_1(\Theta, t) d\Theta$. According to Whitham's procedure,¹⁴ in evaluating this average, the slow time dependence in the integrand is neglected and L_1 is calculated by substituting our two scale representation for X and Y into Eq. (7) and neglecting the time derivative of the slow amplitude. The result is

$$\mathcal{L}_1 = \mathcal{L}_0 - \frac{1}{2} \epsilon \alpha_1 a \cos \Phi, \quad (8)$$

where the unperturbed part is given by $\mathcal{L}_0 = \frac{1}{2} a^2 (\Omega - \omega_0) - \frac{1}{4} \beta \omega_0 a^4$. Formally, the averaged Lagrangian is a function of slow independent variables only, $\mathcal{L}_1 = \mathcal{L}_1(a, \Phi, \Phi_t)$, where the dependence on Φ_t enters via $\Omega = \dot{\Theta}_t = (\Psi + \Phi)_t = \omega_0 + At + \dot{\Phi}_t$ (recall that $A/2\pi$ is the chirp rate of the driving frequency). The next main step of Whitham's approach¹⁴ is to replace the variational principle $\delta \int L(X, X_t, Y, Y_t) dt = 0$ in the original problem by the averaged variational principle $\delta \int \mathcal{L}_1(a, \Phi, \Phi_t) dt = 0$. Then variations with respect to a and Φ yield the desired slow evolution equations. The variation with respect to a gives $a(\Omega - \omega_0) - \beta \omega_0 a^3 - \frac{1}{2} \epsilon \alpha_1 \cos \Phi = 0$, or

$$\Phi_t = \beta \omega_0 a^2 - At + \frac{\epsilon \alpha_1}{2a} \cos \Phi. \quad (9)$$

The variation with respect to Φ yields $(\partial \mathcal{L}_1 / \partial \Omega)_t - \partial \mathcal{L}_1 / \partial \Phi = 0$, i.e.,

$$a_t = \frac{1}{2} \epsilon \alpha_1 \sin \Phi. \quad (10)$$

The set of slow Eqs. (9) and (10) is identical to that derived using a Hamiltonian approach to determine the fundamental autoresonance threshold, as described in Ref. 9. Thus, the current method and the Hamiltonian method are equivalent. Rather than rederiving the fundamental autoresonance threshold, we shall simply quote the results of the Hamiltonian derivation so that we can employ them when we analyze subharmonic autoresonance. The Hamiltonian theory shows that if the system starts out of resonance, the synchro-

nization (phase locking) in the system takes place prior to reaching the linear resonance at $t = 0$, i.e., $\Phi(\text{mod } 2\pi) \rightarrow \pi$ as t approaches zero. Phase locking continues for $t > 0$ and Φ remains near π , providing that the driving amplitude ϵ is above a sharp threshold

$$\epsilon_{\text{th}}^{n=1} = \frac{2}{\alpha_1 \sqrt{\beta \omega_0}} \left(\frac{A}{3} \right)^{3/4}. \quad (11)$$

At the same time the mode amplitude is a monotonically increasing function of time given by substituting $\Phi \approx \pi$ in the right-hand side (RHS) in Eq. (9) and equating it to zero, i.e.,

$$\beta \omega_0 a^2 - At - \frac{\epsilon \alpha_1}{2a} \approx 0. \quad (12)$$

Superimposed on the monotonic solution for a , as given by Eq. (12), are small $O(\epsilon^{1/2})$ autoresonant oscillations. The most critical time for sustaining the resonance is when the driven mode amplitude reaches the value

$$a_{\text{th}} \approx (\frac{1}{2} \epsilon \alpha_1 / \beta \omega_0)^{1/3} \quad (13)$$

at $t \approx 0$. Beyond this time the driving amplitude ϵ can be reduced while still preserving the phase locking. Thus, for ϵ small enough, the threshold phenomenon is indeed a weakly nonlinear effect.

B. $n=2$ subharmonic autoresonance

Now we assume that the driving frequency varies as $\omega_d = \frac{1}{2} \omega_0 + At$, i.e., the drive slowly passes the second order resonance $\omega_d = \frac{1}{2} \omega_0$ at $t = 0$. The linear response of the system at this frequency is nonresonant, and, as mentioned in the Introduction, we look for a frequency doubling of the linear response due to a nonlinear effect, yielding an effective drive at the fundamental frequency. This effective drive will be the source of the autoresonance in the system. The frequency doubling in the evolution equations may come from either the cubic nonlinearity in the unperturbed Lagrangian or the quadratic nonlinearity in its interaction part $-\epsilon S \cos \Psi$. Since the unperturbed Lagrangian [in Eq. (6)] has only even order nonlinear terms, the desired frequency doubling comes only from the s_2 component in the interaction. Thus, the lowest order Lagrangian for studying the $n = 2$ autoresonance differs from that in the fundamental autoresonance case by the addition of a new interaction term, i.e.,

$$L_2 = \frac{1}{2} (XY_t - X_t Y) - \frac{\omega_0}{4} (2\rho^2 + \beta \rho^4) - \epsilon \tilde{S}_2 \cos \Psi, \quad (14)$$

where $\tilde{S}_2 = \alpha_1 s_1 + \alpha_2 s_2$. We seek solutions of the problem of form

$$X = a \cos \Theta + b_x \cos (\frac{1}{2} \Theta + \eta_x), \quad (15)$$

$$Y = a \sin \Theta + b_y \cos (\frac{1}{2} \Theta + \eta_y),$$

where, as in the $n = 1$ case, Θ is the fast angle variable and the first terms are associated with the solution of the unperturbed problem, but we also add the terms describing the

linear response of the system at the subharmonic frequency. The angular frequency $\Omega = \Theta_t$ is again viewed as a slow function of time and we assume the continuing phase locking in the system on the slow time scale, i.e., that the phase mismatches η_x , η_y and $\Phi = \frac{1}{2}\Theta(t) - \Psi(t)$ are bounded and slow. Now we apply Whitham's approach. We observe that the assumed solution is 4π -periodic in the fast angle Θ and, consequently, calculate the averaged Lagrangian in the problem, $\mathcal{L}_2 = (4\pi)^{-1} \int_0^{4\pi} L_2(\Theta, t) d\Theta$. Again, in evaluating the average, the slow time dependence in the integrand is neglected, and $L_2(\Theta, t)$ is calculated by substituting our two scale representation (15) into (14) and neglecting the time derivatives of the slow objects. The resulting, lowest order averaged Lagrangian for studying the $n=2$ subharmonic autoresonance is

$$\mathcal{L}_2 = \mathcal{L}_0 + \mathcal{L}_b + \mathcal{L}_i, \quad (16)$$

where $\mathcal{L}_b = -\frac{1}{4}\omega_0(b_x^2 + b_y^2) + \frac{1}{4}\Omega b_x b_y \sin(\eta_x - \eta_y) - \frac{1}{2}\epsilon\alpha_1 b_x \times \cos(\Phi + \eta_x)$ is the term describing the linear response amplitudes $b_{x,y}$ and slow phases $\eta_{x,y}$, while $\mathcal{L}_i = -\frac{1}{2}\epsilon\alpha_2 a [b_x \cos(\Phi - \eta_x) - b_y \sin(\Phi - \eta_y)]$ represents the interaction due to the component with s_2 in the driving potential, leading to autoresonance in the system in the $n=2$ case, as described above. Now we use \mathcal{L}_2 in the averaged variational principle $\delta \int \mathcal{L}_2(a, b_x, b_y, \eta_x, \eta_y, \Phi, \Phi_t) dt = 0$ and take variations with respect to all the slow independent variables. We proceed from variations with respect to η_x and η_y , yielding

$$\frac{\Omega}{2} b_y \cos(\eta_x - \eta_y) + \epsilon\alpha_1 \sin(\Phi + \eta_x) = \epsilon\alpha_2 a \sin(\Phi - \eta_x),$$

$$\frac{\Omega}{2} b_x \cos(\eta_x - \eta_y) = -\epsilon\alpha_2 a \cos(\Phi - \eta_y).$$

Since, to desired order, $b_{x,y} \sim O(\epsilon)$, the RHS of the last two equations is small for small a . Therefore,

$$\eta_x - \eta_y \approx \pi/2; \quad \Phi + \eta_x \approx 0. \quad (17)$$

The variations with respect to b_x and b_y and the use of Eq. (14) yield two additional lowest order equations,

$$-\omega_0 b_x + \frac{1}{2}\Omega b_y = \epsilon\alpha_1, \quad (18)$$

$$-\omega_0 b_y + \frac{1}{2}\Omega b_x = 0. \quad (19)$$

Assuming that near the resonance $\Omega \approx \omega_0$, we solve these equations for $b_{x,y}$,

$$b_x = -\frac{4\epsilon\alpha_1}{3\omega_0}; \quad b_y = -\frac{2\epsilon\alpha_1}{3\omega_0}. \quad (20)$$

Finally, the remaining variations with respect to a and Φ [recall that $\Phi_t = \frac{1}{2}(\Omega - \omega_0) - At$], and use of Eqs. (17) and (20), yield

$$2\Phi_t = \beta\omega_0 a^2 - 2At - \frac{\epsilon^2\alpha_1\alpha_2}{3\omega_0 a} \cos(2\Phi), \quad (21)$$

$$a_t = -\frac{\epsilon^2\alpha_1\alpha_2}{3\omega_0} \sin(2\Phi). \quad (22)$$

We see that these two variational evolution equations are identical to the set (9) and (10) encountered in the fundamental autoresonance, if, in the latter, we substitute $\Phi \rightarrow 2\Phi + \pi$, $A \rightarrow 2A$, and $\epsilon \rightarrow \epsilon_{\text{eff}} \equiv 2\epsilon^2\alpha_2/3\omega_0$. With these substitutions we can use the same expression Eq. (11) as in the fundamental autoresonance for the threshold of the $n=2$ subharmonic autoresonance, yielding

$$\epsilon_{\text{th}}^{n=2} = \frac{3^{1/8}(\omega_0/\beta)^{1/4}}{\sqrt{\alpha_1\alpha_2}} (2A)^{3/8}. \quad (23)$$

Both s_1 (dipolar) and s_2 (quadrupolar) driving potential components are necessary for $n=2$ subharmonic autoresonance. One can choose different angular extents of the driving sector, or add additional driving sectors having phase-shifted potentials to manipulate these driving components. For example, if the driving sector covers $2\theta_0 = \pi$, the quadrupolar component vanishes and no autoresonance is expected. If $2\theta_0 = \pi/2$, both dipolar and quadrupolar components are present. However, if, in this case, one adds an identical sector opposite to the original driving sector (the corresponding functions s_i for this sector are obtained from the original functions by replacing $X \rightarrow -X$) and the phase of both drives is the same, then the dipolar component of the combined drive vanishes and autoresonance is impossible. If, the second driving sector's phase is shifted by π as compared to the original driving sector, then the combined quadrupolar component of the potential vanishes and autoresonance is again impossible.

One can also analyze more complicated configurations of driving sectors. For instance, the addition of a sector identical to the original one, but rotated by 90° , is equivalent to adding new driving terms obtained from the original ones by swapping $X \rightleftharpoons Y$. If the oscillating potential on the new electrode is shifted by 180° , the first three combined functions s_i become $s_1 = X - Y$, $s_2 = 2(X^2 - Y^2)$, and $s_3 = (X - Y)(X^2 + Y^2 + 4XY)$. With these changes Whitham's technique works as described above. We shall omit the calculations details and just present the results: for $n=1$, the threshold is a factor of $2^{1/2}$ lower than that for the single electrode configuration, while the $n=2$ threshold decreases by a factor of 2.

In the experiment, these sector considerations are complicated by finite length effects. The sectors do not extend the entire length of the plasma and are not centered with respect to the plasma. Consequently, the effect of positive and negative biases applied to a sector are not equal as the different biases attract or repel the plasma, causing the overlap between the sector and plasma to vary. This can introduce new azimuthal harmonics to the drive potential, and new paths to autoresonance, even for sector combinations previously forbidden. In one case these azimuthal harmonics even appear to partially suppress an otherwise allowed path. Nonetheless, the experimental results generally agree with the trends predicted above. Sector combinations predicted to be autoresonant generally are autoresonant, and sector combinations predicted to be nonautoresonant are either not autoresonant or require very large drive voltages to be autoresonant. For example, when the mode is driven with a

single 49° sector 2.45 cm long, the predicted $n=2$ threshold excitation voltage at $A=2\pi\times 4\times 10^5$ Hz/s is $19.5 V_{p-p}$. Experimentally, the required voltage is $27.2 V_{p-p}$, 1.39 times greater. (Note that the data reported in Fig. 2 is for this sector configuration.¹⁵) For two 90° sectors, 3.48 cm long, 90° apart and driven out of phase, the predicted threshold voltage is $3.0 V_{p-p}$. Experimentally, $3.8 V_{p-p}$ is required, a factor of 1.27 times greater. These predictions are not as accurate as those for $n=1$ autoresonance; the small sector requires $0.37 V_{p-p}$ theoretically and $0.32 V_{p-p}$ experimentally, and the dual sectors require $0.074 V_{p-p}$ both theoretically and experimentally. The predictions for the dual sector drive may be more accurate because the drive is bipolar, reducing the affect of the bias on the overlap. Note that these are absolute predictions based on the plasma properties, the trap geometry, and the measured values of ω_0 and β ; there are no free parameters. To make these predictions, we have reduced the coefficients α by the appropriate overlap factor. This overlap factor is simply the ratio of the sector length to the plasma length (5.8 cm), a fact confirmed by a careful calculation of the fields from the sectors via a Fourier–Bessel expansion. The plasma length itself was calculated from the trap geometry and confinement voltages.¹⁶

C. $n=3$ fractional autoresonance

Here we assume that the driving frequency varies as $\omega_d = \frac{1}{3}\omega_0 + At$, i.e., one slowly passes the third order resonance $\omega_d = \frac{1}{3}\omega_0$ at $t=0$. In contrast to the $n=2$ case, where there existed a single path to autoresonance in the system, now we may have three distinct paths and their combinations, depending on which of the s_2 and s_3 components or their combinations are present in the driving potential. The dipolar s_1 component is necessary for all the three paths. Qualitatively, the three routes to $n=3$ subharmonic autoresonance in our system are as follows.

Path I: Suppose the components s_2 and s_3 in the driving potential vanish. Then, near the resonance, the dipolar (s_1) driving component yields nonresonant $O(\epsilon)$ response of the system at the driving frequency $\frac{1}{3}\omega_0$, while the third order nonlinearity in the oscillating system yields $O(\epsilon^3)$ response at the tripled driving frequency, i.e., at ω_0 . It is this resonant third order response which plays the role of an effective drive for exciting autoresonance in the system.

Path II: Here, there exists a nonvanishing s_3 component in the driving potential, but s_2 is still zero. In this case all the ingredients of Path I are present, however, one has an additional effective driving term due to the s_3 component. The nonresonant $O(\epsilon)$ system's response interacts with this component and yields $O(\epsilon^3)$ effective drive at the fundamental (resonant) frequency.

Path III: In this case we add an s_2 component to the driving potential, but assume that the s_3 component is missing. Then one still has all the ingredients of Path I. Now, however, the nonresonant $O(\epsilon)$ response of the system to the dipolar driving component, as well as the resonant response at the fundamental frequency, both enter the s_2 term yielding an $O(\epsilon^2)$ effective drive at frequency $\frac{2}{3}\omega_0$. This effective drive creates a nonresonant $O(\epsilon^2)$ response in the system,

which, in turn, interacts with the quadrupolar s_2 component in the driving potential to produce a new $O(\epsilon^3)$ effective drive, which passes the fundamental frequency ω_0 . Thus, Path III involves a three stage process in creating the resonant effective driving forcing.

We proceed to the analysis of the first two possibilities. Path III adds a new complicating ingredient, namely ϵ_{eff} becomes dependent on the resonant response amplitude itself and we shall not study this case in the present work. As before, the starting point in studying Paths I and II is to write the approximate Lagrangian as

$$L_3 = \frac{1}{2}(XY_t - X_tY) - \frac{\omega_0}{4}(2\rho^2 + \beta\rho^4) - \epsilon\tilde{S}_3 \cos \Psi, \quad (24)$$

where $\tilde{S}_3 = \alpha_1 s_1 + \alpha_3 s_3$ and we set $\alpha_2 = 0$ to avoid the complications associated with Path III. We seek solutions of form

$$X = a \cos \Theta + c_x \cos\left(\frac{1}{3}\Theta + v_x\right), \quad (25)$$

$$Y = a \sin \Theta + c_y \cos\left(\frac{1}{3}\Theta + v_y\right), \quad (26)$$

where the first terms are associated with the fundamental autoresonant solution and, as in the $n=2$ case, we add the terms describing the response of the system at subharmonic frequency. As before, Θ is the fast angle variable. We assume that a , $\Omega = \Theta_t$, $c_{x,y}$ are slow, and phase mismatches v_x , v_y and $\Phi = \frac{1}{3}\Theta(t) - \Psi(t)$ are bounded and slow.

Now, we apply Whitham's approach. We observe that the desired solution is 6π -periodic in fast angle variable and, consequently, calculate the averaged Lagrangian in the problem $\mathcal{L}_3 = (6\pi)^{-1} \int_0^{6\pi} L_3(\Theta, t) d\Theta$. The resulting lowest order averaged Lagrangian describing the $n=3$ subharmonic autoresonance in our system is

$$\mathcal{L}_3 = \mathcal{L}_0 + \mathcal{L}_c + \mathcal{L}_I + \mathcal{L}_{II}. \quad (27)$$

Here $\mathcal{L}_c = -\frac{1}{4}\omega_0(c_x^2 + c_y^2) + \frac{1}{6}\Omega c_x c_y \sin(v_x - v_y) - \frac{1}{2}\epsilon\alpha_1 c_x \cos(\Phi + v_x)$ is the term describing the linear response amplitudes $c_{x,y}$ and slow phases $v_{x,y}$. The terms \mathcal{L}_I and \mathcal{L}_{II} describe Path I and Path II, respectively,

$$\mathcal{L}_I = -\frac{\omega_0 a}{8} [c_x^3 \cos(3v_x) - c_x^2 c_y \sin(2v_x + v_y) + c_x c_y^2 \cos(v_x + 2v_y) - c_y^3 \sin(3v_y)],$$

$$\mathcal{L}_{II} = \frac{3\epsilon\alpha_3 a}{8} [-c_x^2 \cos(\Phi - 2v_x) + c_y^2 \sin(\Phi - 2v_y) + 2c_x c_y \sin(\Phi - v_x - v_y)].$$

Now we use the Lagrangian \mathcal{L}_3 in the averaged variational principle $\delta \int \mathcal{L}_3(a, c_x, c_y, v_x, v_y, \Phi, \Phi_t) dt = 0$ and take variations with respect to all the slow independent variables. We proceed from the variations with respect to v_x and v_y ,

$$\frac{\Omega}{3} c_y \cos(v_x - v_y) + \epsilon\alpha_1 \sin(\Phi + v_x) \approx 0,$$

$$\Omega c_y \cos(v_x - v_y) \approx 0.$$

Therefore,

$$v_x - v_y \approx \pi/2; \quad \Phi + v_x \approx 0. \quad (28)$$

The variations with respect to c_x and c_y and the use of Eq. (28) yield two additional lowest order equations,

$$-\omega_0 c_x + \frac{1}{3}\Omega c_y = \epsilon \alpha_1, \quad (29)$$

$$-\omega_0 c_y + \frac{1}{3}\Omega c_x = 0. \quad (30)$$

Assuming, near the resonance, $\Omega \approx \omega_0$, we solve these equations for $c_{x,y}$,

$$c_x = -\frac{9\epsilon\alpha_1}{8\omega_0}; \quad c_y = -\frac{3\epsilon\alpha_1}{8\omega_0}. \quad (31)$$

Finally, the remaining variations with respect to a and Φ [recall that $\Phi_t = \frac{1}{3}(\Omega - \omega_0) - At$] and use of the equations obtained by varying with respect to $v_{x,y}$ and Eqs. (28) and (30) yield

$$(3\Phi)_t = \beta\omega_0 a^2 - 3At - \frac{\epsilon_{\text{eff}}}{a} \cos(3\Phi), \quad (32)$$

$$a_t = -\epsilon_{\text{eff}} \sin(3\Phi), \quad (33)$$

where $\epsilon_{\text{eff}} = (3^3 \epsilon^3 \alpha_1^2 / 2^7 \omega_0^2)(\alpha_1 - \alpha_3)$. We see that these two slow equations are identical to the set (9) and (10) encountered for the fundamental autoresonance, if in the latter one replaces $\Phi \rightarrow 3\Phi + \pi$, $A \rightarrow 3A$, and $\epsilon\alpha_1/2 \rightarrow \epsilon_{\text{eff}}$. With these substitutions we can again use Eq. (11) for finding the threshold of the $n=3$ subharmonic autoresonance in our system,

$$\epsilon_{\text{th}}^{n=3} = \frac{2^{7/3} \omega_0^{1/2} A^{1/4}}{3\beta^{1/6} \alpha_1 (1 - \alpha_3/\alpha_1)^{1/3}}. \quad (34)$$

This completes our discussion of the $n=3$ subharmonic autoresonance of the diocotron mode.

III. CONCLUSIONS

(A) We have studied subharmonic autoresonant excitation and control of the $l=1$ diocotron mode. The subharmonic autoresonance is excited when the n^{th} harmonic ($n=2,3,\dots$) of the chirped driving frequency $\omega_d(t)$ passes the linear diocotron mode frequency. The reason for the subharmonic autoresonance in the system is the ability of n^{th} order nonlinearities of the driven diocotron mode and/or of the external oscillating field to serve as an effective drive at the fundamental frequency $\omega_0 \approx n\omega_d(t)$. This effective drive plays a role similar to that of a resonant fundamental harmonic drive in exciting the fundamental autoresonance in the system. Thus, understanding of subharmonic autoresonance reduces to the study of higher order nonlinear driven response in the system.

(B) For a given chirp rate of the driving frequency, entering subharmonic autoresonance requires that the driving amplitude exceeds a sharp threshold [see Eq. (1)]. Below the threshold the passage through the resonance does not lead to a significant excitation of the mode. In contrast, above the threshold the system phase locks to the drive and the synchronization in the system continues despite the variation of

the driving frequency. As a result, the mode amplitude may increase significantly as the system self-adjusts its nonlinear response to stay in resonance with the drive.

(C) Because it is a higher order effect, the subharmonic autoresonance requires larger driving amplitudes, but lower driving frequencies as compared to the fundamental ($n=1$) autoresonance. The theoretical description of the process becomes increasingly complex as the order n of resonance increases and new paths to autoresonance associated with various order nonlinearities of the mode and/or the driving field come into play.

(D) We have developed the theory of the subharmonic autoresonance threshold for $n=2$ and a part of possible paths of $n=3$ case. The theory is based on Whitham's averaged variational principle, a convenient approach for studying slow, phase-locked, autoresonant driven solutions in our system.

(E) The results of the theory were compared with the experiments for $n=2$ in a variety of driving configurations. The agreement between the theory and the experiment was very good not only in terms of the predicted 3/8 power law for the threshold vs chirp rate, but also in absolute measured threshold values, found to be within 40% from those predicted by the theory. We have also experimentally studied excitation of higher order ($n=3,4,5$) subharmonic autoresonance in the system. The measured dependence of the threshold on the chirp rate for entering these higher order subharmonic autoresonances was found to be in excellent agreement with the theoretically predicted $3/4n$ exponent in the power law.

(F) It seems interesting to extend the study of both the fundamental and subharmonic autoresonance in non-neutral plasmas to other oscillatory degrees of freedom, an example being the Kelvin mode. Also, studying the multifrequency autoresonance, where one simultaneously excites and controls a combination of oscillatory modes, constitutes a challenging goal for future studies. These investigations would have a direct impact on similar problems in the driven dynamics of two-dimensional ideal fluids, where vortices are analogs of non-neutral plasma columns, and oscillating straining flows correspond to the chirped frequency driving fields in plasma experiments.

ACKNOWLEDGMENTS

This work was supported by the U.S.–Israel Binational Science Foundation, and the Office of Naval Research.

¹M. S. Livingston, *High-Energy Particle Accelerators* (Interscience, New York, 1954).

²B. Meerson and L. Friedland, *Phys. Rev. A* **41**, 5233 (1990).

³W. K. Liu, B. Wu, and J. M. Yuan, *Phys. Rev. Lett.* **75**, 1292 (1995).

⁴G. Cohen and B. Meerson, *Phys. Rev. E* **47**, 967 (1993).

⁵I. Aranson, B. Meerson, and T. Tajima, *Phys. Rev. A* **45**, 7500 (1992).

⁶L. Friedland and A. G. Shagalov, *Phys. Rev. Lett.* **81**, 4357 (1998).

⁷L. Friedland, *Phys. Rev. E* **59**, 4106 (1999).

⁸J. Fajans, E. Gilson, and L. Friedland, *Phys. Rev. Lett.* **82**, 4444 (1999).

⁹J. Fajans, E. Gilson, and L. Friedland, *Phys. Plasmas* **6**, 4497 (1999).

¹⁰J. H. Malmberg, C. F. Driscoll, B. Beck, D. L. Eggleston, J. Fajans, K. Fine, X. P. Huang, and A. W. Hyatt, in *Non-neutral Plasma Physics*, edited by C. Roberson and C. Driscoll (American Institute of Physics, New York, 1988), Vol. AIP 175, p. 28.

¹¹L. Friedland, Phys. Rev. E (in press).

¹²The sine wave generator used to produce the driving signal could have confused our results by generating unwanted harmonic components that excite the fundamental autoresonance directly. To rule out this possibility, we measured the amplitudes of the harmonics, and found that in all cases, they were comfortably below the fundamental threshold.

¹³K. S. Fine and C. F. Driscoll, Phys. Plasmas **5**, 601 (1998).

¹⁴G. B. Whitham, *Linear and Nonlinear Waves* (Wiley, New York, 1974), p. 472.

¹⁵More precisely, some of the data in Fig. 2 required stronger drives than could be obtained with a single 49° sector. For these data, we used one or two 90° sectors, and scaled the data appropriately by overlapping data taken with the 49° and the 90° sectors in their common range.

¹⁶Rather than use a full numeric simulation to calculate the plasma length, we the simplification that the plasma ends where the vacuum fields equal half the plasma central potential. This simplification is based on calculations in A. J. Peurrung and J. Fajans, Phys. Fluids B **2**, 693 (1990), and has proven to be accurate in the past.